Journal of
Mechanics of
Materials and Structures

msp

msp

WORST-CASE LOAD IN PLASTIC LIMIT
ANALYSIS OF FRAME STRUCTURES

Yoshihiro Kanno

This paper addresses the plastic limit analysis of a frame structure under uncertainty in the external load. Given a bounded set in which an external load can vary, we attempt to find the worst load that minimizes the limit load factor. It is shown that this problem can be formulated as a mixed-integer linear programming problem. The global optimal solution of this optimization problem can be found by using an existing algorithm, e.g., a branch-and-cut method. Guaranteed convergence to a global optimal solution is important because it implies that the proposed method yields neither overestimation nor underestimation in this uncertainty analysis problem. Two numerical examples illustrate that the worst scenario problem can be solved with modest computational effort. They also show that not only does the limit load factor depend on the level of uncertainty in the external load, but the collapse mode as well.

1. Introduction

This paper presents a numerical method for finding the worst-case loading in plastic limit analysis of a frame structure. Possibilistic (or bounded-but-unknown) models, rather than probabilistic models, are employed to represent the uncertainty in the external load. Then the worst scenario is defined as the external load with which the plastic limit load factor attains the minimum value.

Since real-world structures inevitably encounter various uncertainties stemming from manufacturing variability, aging, limitation of knowledge of input disturbance, etc., the concept of robustness to uncertainty is central in structural design [Zang et al. 2005; Beyer and Sendhoff 2007; Schuëller and Jensen 2008; Valdebenito and Schuëller 2010]. Probabilistic and possibilistic methods for analysis and design of structures under uncertainties have been compared in the literature [Langley 2000; Nikolaidis et al. 2004]. If a reliable statistical property of uncertainty is available, then probabilistic reliability analysis can be performed. In contrast, a possibilistic model of uncertainty might be applicable to problems without reliable stochastic information, because it requires only bounds for the input data to define the uncertainty and hence is often less information intensive. In this case, the key is to analyze the worst scenario, that is, the most severe scenario among a given set of scenarios, in order to assess the robustness of the structure [Ben-Haim and Elishakoff 1990; Hlaváček et al. 2004; Ben-Haim 2006]. The problem of finding the worst scenario, called the *worst scenario problem*, is formulated as an optimization problem, and the worst scenario corresponds to its optimal solution. It is worth noting that the worst scenario

problem should be solved by an algorithm with guaranteed global convergence, because, obviously, a local (but not global) optimal solution is not necessarily the worst scenario. In this paper attention is focused on development of a global optimization method for the worst scenario problem.

There exists a vast literature on numerical methods for worst scenario problems. The so-called convex modeling approach [Ben-Haim and Elishakoff 1990] is one of the best-known methods and has been applied in many areas. Interval arithmetic, originally developed for finding bounds on round-off errors [Neumaier 1990; Alefeld and Mayer 2000], has also been applied to various problems in mechanics [McWilliam 2001; Chen et al. 2002; De Gersem et al. 2007; Neumaier and Pownuk 2007; Degrauwe et al. 2010]. It finds a conservative bound, i.e., an outer bound, for the response of a structural system with uncertainty; for details, as well as surveys on other nonprobabilistic uncertainty analyses, see [Moens and Vandepitte 2005], [Möller and Beer 2008], and [Moens and Hanss 2011]. Since the worst scenario problem is formulated as an optimization problem, it might be natural to use an optimization algorithm for finding the worst scenario. However, direct use of a conventional nonlinear programming approach is not guaranteed to provide a conservative solution, unless the worst scenario problem is convex. Also, metaheuristics including genetic algorithms, which have been applied to complex engineering systems [Biondini et al. 2004; Catallo 2004], do not necessarily converge to the global optimal solution and hence their solutions are on the unsafe side in general. For nonconvex worst scenario problems, two nontraditional approaches have been recently developed to ensure conservativeness: one is to construct a convex approximation problem that provides a conservative bound, while the other is to reformulate the original worst scenario problem to another equivalent optimization problem for which an algorithm with guaranteed convergence to the global optimal solution is available. Taking the former approach, semidefinite programming approximations have been developed for static problems [Kanno and Takewaki 2006; 2008; Guo et al. 2009; 2011] and a dynamic steady-state problem [Kanno and Takewaki 2009]. With the latter approach, *mixed-integer linear programming* (MILP) formulations have been studied for static analysis [Guo et al. 2008] and plastic limit analysis of trusses [Kanno and Takewaki 2007; Kanno 2012]. Although this MILP approach is applicable only in some specific cases, its distinguishing feature is guaranteed convergence to the exact worst case; in other words, it returns neither overestimation nor underestimation.

In [Kanno and Takewaki 2007] an MILP formulation was developed to solve the worst scenario problem in the plastic limit analysis of a truss, where the external load was considered uncertain and assumed to be included in a given convex set. In a continuation of this work, we extend the result to frame structures. It is shown that the worst scenario problem of a frame structure can also be converted to an MILP problem, provided that the yield surface is represented by a piecewise linear function of the axial force and the end moment. The global optimal solution of an MILP problem can be found with, e.g., a branch-and-cut algorithm; several well-developed software packages, e.g., Gurobi Optimizer [Gurobi 2013] and CPLEX [IBM ILOG 2011], are available for this purpose. Guaranteed convergence to a global optimal solution implies that the exact worst case can be found by the proposed method. Since we restrict ourselves to the case of piecewise linear yield functions, the problem for frame structures in this paper is not much different from the one for trusses in [Kanno and Takewaki 2007] from a mathematical point of view. For instance, the limit analysis problems of both structures can be formulated as *linear programming* (LP) problems, although, due to the effect of interaction between the axial force and the end moment, the formulation for frame structures is slightly more complicated. From an engineering

point of view, however, limit analysis that can deal with frame structures has more significance than analysis that is limited to trusses. Also, in [Kanno and Takewaki 2007] the worst-case load is found by solving a MILP problem with generation of some disjunctive cuts and a subsequent naive branch-and-bound method with depth-first search. Accordingly, the size of problems that could be solved was limited. In contrast, in this paper the efficiency of a commercial software package, CPLEX [IBM ILOG 2011], is examined.

Note that an MILP problem is a minimization, or maximization, problem of a linear function under linear constraints, where some of the variables are constrained to be integers and the remaining variables are considered to be continuous real variables. Specifically, the MILP problem solved in this paper is of the form

$$\text{Minimize } c^{\mathrm{T}}x + g^{\mathrm{T}}y \tag{1a}$$

$$\text{subject to } Ax + Fy = b, \tag{1b}$$

$$x \in \{0, 1\}^n, \tag{1c}$$

$$y \geq 0. \tag{1d}$$

Here $x \in \mathbb{R}^n$ and $y \in \mathbb{R}^p$ are variables to be optimized, $A \in \mathbb{R}^{m \times n}$ and $F \in \mathbb{R}^{m \times p}$ are constant matrices, and $c \in \mathbb{R}^n$, $g \in \mathbb{R}^p$, and $b \in \mathbb{R}^m$ are constant vectors. Problem (1) is also called a mixed 0-1 linear programming problem, because the integer variables, $x_1, \ldots, x_n$, are restricted to being either 0 or 1. If we replace the binary constraints, (1c), with linear inequality constraints, $0 \leq x_j \leq 1$ $(j = 1, \ldots, n)$, then the resulting relaxation problem is an LP problem. By virtue of this property, a global solution of (1) can be found by enumerating all possible realizations of binary variables, $x_1, \ldots, x_n$. To make this enumeration more efficient, a branch-and-bound method discards hopeless candidates by making use of upper and lower bounds on the objective function. Efficient software packages for solving MILP usually implement a branch-and-cut method, which is a combination of a branch-and-bound method and a cutting-plane method. A cutting-plane method iteratively generates valid inequalities of (1), called cuts, to refine the feasible set of the relaxation problem; see, for example, [Wolsey 1998], [Faigle et al. 2002], and [Aardal et al. 2005] for fundamentals of MILP and related algorithms.

Limit analysis under probabilistic uncertainties has been studied within several frameworks. For evaluating the probability of plastic collapse, the first and second-order methods in reliability analysis were employed in [Bjerager 1989; Wang et al. 1994; Staat and Heitzer 2003; Trân et al. 2009] and the stochastic programming approach was applied in [Sikorski and Borkowski 1990; Marti and Stoeckl 2004; Marti 2008]. When the yield strengths are assumed to be stochastic variables, the conditional probability of collapse, that is, the probability of plastic collapse under the given load, was evaluated in [Caddemi et al. 2002; Alibrandi and Ricciardi 2008]. The classical optimal plastic design is to find a structural design that minimizes the total structural volume under the constraint on the plastic limit load factor. For this problem, fuzzy LP approaches were proposed in [Munro and Chuang 1986; Jung and Pulmano 1996], where uncertainty was modeled by employing fuzzy set theory. Unlike those studies, this paper addresses possibilistic uncertainty models in the external load and attempts to find the worst loading scenario.

This paper is organized as follows. Section 2 prepares LP formulations for the conventional limit analysis of frame structures. Section 3 presents our main result: The worst scenario problem in limit

analysis is reformulated to an MILP problem. Two numerical experiments are performed in Section 4. We conclude in Section 5. Proofs of propositions appear in the Appendix.

A few words regarding notation. All vectors are assumed to be column vectors. The $(m+n)$-dimensional column vector $(\boldsymbol{v}^{\mathrm{T}}, \boldsymbol{x}^{\mathrm{T}})^{\mathrm{T}}$ consisting of $\boldsymbol{v} \in \mathbb{R}^m$ and $\boldsymbol{x} \in \mathbb{R}^n$ is often written simply as $(\boldsymbol{v}, \boldsymbol{x})$. For two vectors $\boldsymbol{x} = (x_1, \ldots, x_n)^{\mathrm{T}} \in \mathbb{R}^n$ and $\boldsymbol{y} = (y_1, \ldots, y_n)^{\mathrm{T}} \in \mathbb{R}^n$, we write $\boldsymbol{x} \geq \boldsymbol{y}$ if $x_i \geq y_i$ $(i = 1, \ldots, n)$. Particularly, $\boldsymbol{x} \geq \boldsymbol{0}$ means $x_i \geq 0$ $(i = 1, \ldots, n)$. The ℓ^1-norm and the ℓ^∞-norm of vector $\boldsymbol{x} \in \mathbb{R}^n$ are defined by

$$\|\boldsymbol{x}\|_1 = \sum_{i=1}^{n} |x_i|, \quad \|\boldsymbol{x}\|_\infty = \max_{i=1,\ldots,n} |x_i|.$$

We use $\boldsymbol{1} = (1, 1, \ldots, 1)^{\mathrm{T}}$ to denote the all-ones vector.

2. Fundamentals of limit analysis

This section summarizes LP formulations of the conventional limit analysis of frame structures. Section 2A describes the yield conditions that we adopt in this paper. Section 2B presents an LP formulation of the lower bound principle. The dual problem which corresponds to the upper bound principle is presented in Section 2C.

2A. *Yield conditions.* In this paper we consider only planar frame structures for simplicity. Spatial frames can be dealt with in the same manner.

Suppose that the frame structure consists of E beam elements. Let $\boldsymbol{s}_e \in \mathbb{R}^3$ denote the generalized stress vector of member e $(e = 1, \ldots, E)$. For example, the components of $\boldsymbol{s}_e \in \mathbb{R}^3$ can be chosen as

$$\boldsymbol{s}_e = \begin{bmatrix} q_e \\ m_e^{(1)} \\ m_e^{(2)} \end{bmatrix},$$

where q_e is the axial force and $m_e^{(1)}$ and $m_e^{(2)}$ are the end moments. The yield condition of member e is assumed to be written in the form

$$\|\boldsymbol{A}_{e,j} \boldsymbol{s}_e\|_1 \leq R_{e,j}, \quad j = 1, \ldots, J. \tag{2}$$

Two concrete examples of (2) are given in Examples 2.1 and 2.2.

Example 2.1. Suppose that the dependence of the yield condition on the shear force is negligible. Consider a piecewise linear yield surface in Figure 1, which involves the simple effect of interaction between the axial force and the end moment. This yield condition is written as

$$\frac{|q_e|}{q_e^{\mathrm{y}}} + \frac{|m_e^{(1)}|}{m_e^{\mathrm{y}}} \leq 1, \tag{3a}$$

$$\frac{|q_e|}{q_e^{\mathrm{y}}} + \frac{|m_e^{(2)}|}{m_e^{\mathrm{y}}} \leq 1, \tag{3b}$$
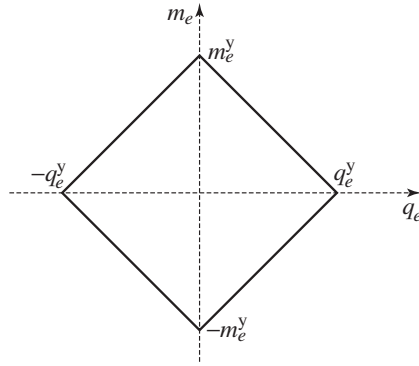
Figure 1. Yield surface of a beam element in Example 2.1.

where q_e^{y} and m_e^{y} are admissible absolute values of the axial force and the end moment, respectively. Let $J = 2$. Define matrices $\boldsymbol{A}_{e,j}$ $(j = 1, 2)$ by

$$\boldsymbol{A}_{e,1} = \begin{bmatrix} 1/q_e^{\mathrm{y}} & 0 & 0 \\ 0 & 1/m_e^{\mathrm{y}} & 0 \end{bmatrix}, \quad \boldsymbol{A}_{e,2} = \begin{bmatrix} 1/q_e^{\mathrm{y}} & 0 & 0 \\ 0 & 0 & 1/m_e^{\mathrm{y}} \end{bmatrix},$$

and constants $R_{e,j}$ $(j = 1, 2)$ by

$$R_{e,1} = R_{e,2} = 1.$$

Then yield condition (3) is written in the form of (2).

Example 2.2. As a piecewise linear model slightly more complex than Example 2.1, consider the yield surface depicted in Figure 2. Here $\kappa \in (1, \sqrt{2})$ is a constant.[1] This yield condition is formulated as

$$\frac{|q_e|}{\kappa q_e^{\mathrm{y}}} + \frac{|m_e^{(1)}|}{\kappa m_e^{\mathrm{y}}} \leq 1, \quad \left| \frac{q_e}{2q_e^{\mathrm{y}}} + \frac{m_e^{(1)}}{2m_e^{\mathrm{y}}} \right| + \left| \frac{-q_e}{2q_e^{\mathrm{y}}} + \frac{m_e^{(1)}}{2m_e^{\mathrm{y}}} \right| \leq 1, \tag{4a}$$

$$\frac{|q_e|}{q_e^{\mathrm{y}}} + \frac{|m_e^{(2)}|}{m_e^{\mathrm{y}}} \leq 1, \quad \left| \frac{q_e}{2q_e^{\mathrm{y}}} + \frac{m_e^{(2)}}{2m_e^{\mathrm{y}}} \right| + \left| \frac{-q_e}{2q_e^{\mathrm{y}}} + \frac{m_e^{(2)}}{2m_e^{\mathrm{y}}} \right| \leq 1. \tag{4b}$$

Let $J = 4$ and define $\boldsymbol{A}_{e,j}$ by

$$\boldsymbol{A}_{e,1} = \begin{bmatrix} 1/\kappa q_e^{\mathrm{y}} & 0 & 0 \\ 0 & 1/\kappa m_e^{\mathrm{y}} & 0 \end{bmatrix}, \quad \boldsymbol{A}_{e,3} = \begin{bmatrix} 1/2q_e^{\mathrm{y}} & 1/2m_e^{\mathrm{y}} & 0 \\ -1/2q_e^{\mathrm{y}} & 1/2m_e^{\mathrm{y}} & 0 \end{bmatrix}, \tag{5a}$$

$$\boldsymbol{A}_{e,2} = \begin{bmatrix} 1/\kappa q_e^{\mathrm{y}} & 0 & 0 \\ 0 & 0 & 1/\kappa m_e^{\mathrm{y}} \end{bmatrix}, \quad \boldsymbol{A}_{e,4} = \begin{bmatrix} 1/2q_e^{\mathrm{y}} & 0 & 1/2m_e^{\mathrm{y}} \\ -1/2q_e^{\mathrm{y}} & 0 & 1/2m_e^{\mathrm{y}} \end{bmatrix}, \tag{5b}$$

and $R_{e,j}$ by

$$R_{e,1} = R_{e,2} = R_{e,3} = R_{e,4} = 1.$$

Then (4) is expressed by (2).

---

[1]If $\kappa \leq 1$, then (4) is reduced to (3) in Example 2.1. On the other hand, if $\kappa \geq \sqrt{2}$, (4) is reduced to a box constraint, i.e., $|q_e| \leq q_e^{\mathrm{y}}$, $|m_e^{(1)}| \leq m_e^{\mathrm{y}}$, and $|m_e^{(2)}| \leq \mu_e^{\mathrm{y}}$, which does not involve interaction between the axial force and the end moment.
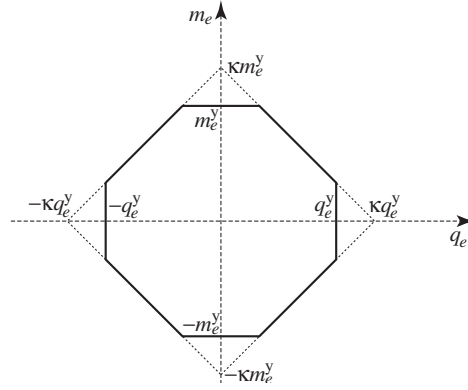
Figure 2. Piecewise linear yield surface in Example 2.2.

2B. *Lower bound principle.* Suppose that the external load consists of a constant part, denoted by p, and a proportionally increasing part, expressed as λf. The constant vector $f \in \mathbb{R}^d \setminus \{0\}$ is called the *reference load*, where d is the number of displacement degrees of freedom. The parameter $\lambda \in \mathbb{R}$ is called the *load factor*. The force-balance equation is written as

$$Hs = p + \lambda f, \tag{6}$$

where $H \in \mathbb{R}^{d \times 3E}$ is the equilibrium matrix and $s = (s_1^{\mathrm{T}}, \ldots, s_E^{\mathrm{T}}) \in \mathbb{R}^{3E}$.

From the lower bound principle, the limit load factor, denoted $\bar{\lambda}$, is defined as the maximum value of λ under the yield condition (2) and the force-balance equation (6). Specifically, $\bar{\lambda}$ is the optimal value of the following optimization problem:

$$
\begin{aligned}
&\text{Maximize } \lambda \text{ over } \lambda, s \\
&\text{subject to} \quad Hs = p + \lambda f, \\
&\qquad\qquad \|A_{e,j} T_e s\|_1 \le R_{e,j}, \quad e = 1, \ldots, E, \ j = 1, \ldots, J.
\end{aligned} \tag{7}
$$

Here for each $e = 1, \ldots, E$, $T_e \in \mathbb{R}^{3 \times 3E}$ is a constant matrix satisfying

$$T_e s = \begin{bmatrix} q_e \\ m_e^{(1)} \\ m_e^{(2)} \end{bmatrix}.$$

Throughout the paper we assume that problem (7) is feasible and its optimal value is bounded above.

Remark 2.3. Problem (7) can be solved as an LP problem. To see this, it suffices to show that constraint $\|A_{e,j} T_e s\|_1 \le R_{e,j}$ can be converted to some linear inequality constraints. We begin with the following slightly simpler form:

$$\|x\|_1 = \sum_{i=1}^{n} |x_i| \le b. \tag{8}$$

For each $i = 1, \ldots, n$, let ξ_i be an additional variable that serves as an upper bound for $|x_i|$, that is, $|x_i| \le \xi_i$. This relation is written as the following linear inequality constraints:

$$-\xi_i \le x_i \le \xi_i, \quad i = 1, \ldots, n. \tag{9}$$

Then $\sum_{i=1}^{n} \xi_i$ becomes an upper bound for $\|x\|_1$. Therefore, (8) is rewritten as (9) and

$$\sum_{i=1}^{n} \xi_i \leq b. \tag{10}$$

In the same manner, the constraint $\|A_{e,j}T_e s\|_1 \leq R_{e,j}$ in problem (7) can be converted to finitely many linear inequality constraints. Let $|A_{e,j}T_e s|$ be a vector of the absolute values of the components of $A_{e,j}T_e s$. Use a vector of additional variables, $\boldsymbol{\eta}_{e,j}$, to express upper bounds for components of $|A_{e,j}T_e s|$, that is, $|A_{e,j}T_e s| \leq \boldsymbol{\eta}_{e,j}$. Then, the sum of components of $\boldsymbol{\eta}_{e,j}$, that is, $\mathbf{1}^T\boldsymbol{\eta}_{e,j}$, serves as an upper bound for $\|A_{e,j}T_e s\|_1$. Therefore, problem (7) can be rewritten as

$$
\begin{aligned}
&\text{Maximize } \lambda \text{ over } \lambda, s, \boldsymbol{\eta} \\
&\text{subject to} \quad \boldsymbol{H}s = \boldsymbol{p} + \lambda \boldsymbol{f}, \\
&\qquad\qquad R_{e,j} \geq \mathbf{1}^T\boldsymbol{\eta}_{e,j}, \qquad\qquad j = 1, \ldots, J, \quad e = 1, \ldots, E, \\
&\qquad\qquad -\boldsymbol{\eta}_{e,j} \leq A_{e,j}T_e s \leq \boldsymbol{\eta}_{e,j}, \quad j = 1, \ldots, J, \quad e = 1, \ldots, E,
\end{aligned}
\tag{11}
$$

which is clearly an LP problem.

2C. *Upper bound principle.* In Section 2B we have formulated the limit analysis problem, (7), based on the lower bound principle. The upper bound principle corresponds to the dual problem. In Section 3 we shall use the upper bound principle to formulate the worst scenario problem.

Let $\boldsymbol{u} \in \mathbb{R}^d$ denote the vector of nodal displacements. We use $z_{e,j}$ to denote the generalized strain vector that is conjugate to $A_{e,j}T^T s$. The dual problem of problem (7) can be formulated in variables $\boldsymbol{u}$, $\gamma_{e,j}$, and $z_{e,j}$ ($e = 1, \ldots, E$ and $j = 1, \ldots, J$) as

$$
\begin{aligned}
&\text{Minimize } -\boldsymbol{p}^T\boldsymbol{u} + \sum_{e=1}^{E}\sum_{j=1}^{J} R_{e,j}\gamma_{e,j} \text{ over } \boldsymbol{u}, \boldsymbol{\gamma}, \boldsymbol{z} \\
&\text{subject to} \quad \boldsymbol{f}^T\boldsymbol{u} = 1, \\
&\qquad\qquad \sum_{e=1}^{E}\sum_{j=1}^{J} (A_{e,j}T_e)^T z_{e,j} = \boldsymbol{H}^T\boldsymbol{u}, \\
&\qquad\qquad \gamma_{e,j} \geq \|z_{e,j}\|_\infty, \quad e = 1, \ldots, E, \ j = 1, \ldots, J.
\end{aligned}
\tag{12}
$$

See Section A.1 for the derivation of (12). At the optimal solution we obtain $\gamma_{e,j} = \|z_{e,j}\|_\infty$ ($e = 1, \ldots, E$; $j = 1, \ldots, J$), because $R_{e,j}\gamma_{e,j}$ is minimized under constraint $\gamma_{e,j} \geq \|z_{e,j}\|_\infty$. Thus $\gamma_{e,j}$ becomes equal to the sum of the absolute values of the generalized plastic strain at the j-th end of member e.

Remark 2.4. Problem (12) can be solved as an LP problem. Indeed, the constraint $\gamma_{e,j} \geq \|z_{e,j}\|_\infty$ of (12) can be rewritten as

$$-\gamma_{e,j}\mathbf{1} \leq z_{e,j} \leq \gamma_{e,j}\mathbf{1},$$

which is a system of linear inequalities.

With reference to Remarks 2.3 and 2.4, the duality theory of LP implies that problems (7) and (12) share the same optimal value, because we assume that (7) has an optimal solution. In short, the optimal value of (12) is equal to $\bar{\lambda}$.

3. Worst scenario detection

In Section 3A we formally define the worst-case load, where the ℓ^∞-norm of uncertain parameters is bounded. Section 3B shows that the worst-case load can be obtained as the optimal solution of an MILP problem. This problem can be solved globally by using an existing algorithm, e.g., a branch-and-bound method. Section 3C explores the worst scenario problem in which the ℓ^1-norm of uncertain parameters is bounded.

3A. *Definition of worst-case load.* As summarized in Section 2, the limit load factor, $\bar{\lambda}$, of a given frame structure is determined when the load vectors, $\boldsymbol{p}$ and $\boldsymbol{f}$, are specified. In the following, $\bar{\lambda}$ is considered a function of $\boldsymbol{p}$, i.e., $\bar{\lambda}(\boldsymbol{p})$, while $\boldsymbol{f}$ is assumed to be fixed. In other words, we suppose that only $\boldsymbol{p}$ is uncertain.

Uncertainty in $\boldsymbol{p}$ is modeled as follows. Let $\tilde{\boldsymbol{p}} \in \mathbb{R}^d$ denote the nominal value, or the best estimate, of $\boldsymbol{p}$. We use an unknown vector $\boldsymbol{\zeta} \in \mathbb{R}^L$ ($L \leq d$) to express uncertainty in $\boldsymbol{p}$. Suppose that $\boldsymbol{p}$ depends on $\boldsymbol{\zeta}$ affinely as

$$\boldsymbol{p} = \tilde{\boldsymbol{p}} + \boldsymbol{Q}\boldsymbol{\zeta} \tag{13}$$

and that the norm of $\boldsymbol{\zeta}$ is known to be bounded. Here $\boldsymbol{Q} \in \mathbb{R}^{d \times L}$ is a constant matrix satisfying rank $\boldsymbol{Q} = L$. The unknown vector $\boldsymbol{Q}\boldsymbol{\zeta} \in \mathbb{R}^d$ corresponds to the difference between the actual load, $\boldsymbol{p}$, and the estimated load, $\tilde{\boldsymbol{p}}$. The number of independently varying components of uncertain load, $\boldsymbol{Q}\boldsymbol{\zeta}$, is L. The set of all such loading scenarios is given by

$$P(\alpha, \tilde{\boldsymbol{p}}) = \{\tilde{\boldsymbol{p}} + \boldsymbol{Q}\boldsymbol{\zeta} \mid \|\boldsymbol{\zeta}\|_\infty \leq \alpha\}, \tag{14}$$

where $\alpha \geq 0$ is a constant. We call $P(\alpha, \tilde{\boldsymbol{p}})$ the *uncertainty set* of the load. Parameter α, called the *uncertainty parameter*, expresses the level of uncertainty in the following sense [Ben-Haim 2006]:

(i) $P(0, \tilde{\boldsymbol{p}}) = \{\tilde{\boldsymbol{p}}\}$ and

(ii) $\alpha \leq \alpha'$ implies $P(\alpha, \tilde{\boldsymbol{p}}) \subseteq P(\alpha', \tilde{\boldsymbol{p}})$.

Namely, (i) only the nominal loading scenario is considered at $\alpha = 0$ and (ii) the range of possible scenarios of external loads increases as α increases.

For given α and $\tilde{\boldsymbol{p}}$, vector $\boldsymbol{p}$ takes any value in $P(\alpha, \tilde{\boldsymbol{p}})$. The limit load factor in the worst scenario is then defined as the minimum value of $\bar{\lambda}(\boldsymbol{p})$. Formally, the *worst-case limit load factor*, denoted $\lambda_{\min}(\alpha, \tilde{\boldsymbol{p}})$, for a given α and $\tilde{\boldsymbol{p}}$ is defined by

$$\lambda_{\min}(\alpha, \tilde{\boldsymbol{p}}) = \min\{\bar{\lambda}(\boldsymbol{p}) \mid \boldsymbol{p} \in P(\alpha, \tilde{\boldsymbol{p}})\}. \tag{15}$$

Accordingly, the worst-case load, denoted $\boldsymbol{p}_{\mathrm{w}}$, is defined as the optimal solution of this maximization problem, i.e.,

$$\boldsymbol{p}_{\mathrm{w}} \in \arg\min\{\bar{\lambda}(\boldsymbol{p}) \mid \boldsymbol{p} \in P(\alpha, \tilde{\boldsymbol{p}})\}. \tag{16}$$

It is worth noting that this optimization problem should be solved by an algorithm with guaranteed convergence to a global optimal solution, because, obviously, a local (but not global) optimal solution is not the most severe scenario. In Section 3B, we shall reduce problem (16) to an MILP problem, the global optimal solution of which can be found with an existing algorithm.

Remark 3.1. Since both the set of admissible (generalized) stress vectors and the set of uncertain external loads are polytopes, the worst-case load, p_w, in (16) can be found by enumerating all vertices of polytope $P(\alpha, \tilde{p})$. Actually this is similar to what is often done in shakedown analysis; see, for example, [Polizzotto 1982], [Ngo and Tin-Loi 2007], [Simon and Weichert 2012], and references therein. However, enumeration of all vertices immediately becomes inexecutable when L, i.e., the number of independently varying components of the uncertain load, increases, because $P(\alpha, \tilde{p})$ has 2^L vertices. For instance, in the numerical example of Section 4A we suppose $L = 55$, which results in $2^{55} \simeq 3.6 \times 10^{16}$ vertices. We use an MILP approach to deal with such problems.

Remark 3.2. The notion of the worst-case load has been introduced as the loading scenario when uncertainty is pernicious. Alternatively, uncertainty may be propitious, in the sense that the limit load factor can possibly increase with some p belonging to $P(\alpha, \tilde{p})$. Finding such a case, called the opportune case by some authors [Ben-Haim 2006], together with the worst case will provide us with the range of the structural response under uncertainty. The opportune-case limit load factor is defined by

$$\lambda_{\max}(\alpha, \tilde{p}) = \max\{\bar{\lambda}(p) \mid p \in P(\alpha, \tilde{p})\}, \tag{17}$$

where minimization in (15) has been replaced by maximization. Computing $\lambda_{\max}(\alpha, \tilde{p})$ is much easier than computing $\lambda_{\min}(\alpha, \tilde{p})$. Recall that, for a fixed p, the lower bound principle is given by problem (14), the optimal value of which is $\bar{\lambda}(p)$. From this and the definition in (14) of $P(\alpha, \tilde{p})$, we immediately see that $\lambda_{\max}(\alpha, \tilde{p})$ is the optimal value of the following problem:

$$
\begin{aligned}
&\text{Maximize } \lambda \text{ over } \lambda, s, \zeta \\
&\text{subject to} \quad Hs = \tilde{p} + Q\zeta + \lambda f, \\
&\qquad\qquad \|A_{e,j} T_e s\|_1 \le R_{e,j}, \qquad e = 1, \ldots, E, \ j = 1, \ldots, J, \\
&\qquad\qquad \alpha \ge \|\zeta\|_\infty.
\end{aligned}
\tag{18}
$$

Here λ, s, and ζ are variables to be optimized. In a manner similar to Remark 2.3, we can rewrite problem (18) as

$$
\begin{aligned}
&\text{Maximize } \lambda \text{ over } \lambda, s, \zeta, \eta \\
&\text{subject to} \quad Hs = \tilde{p} + Q\zeta + \lambda f, \\
&\qquad\qquad R_{e,j} \ge \mathbf{1}^T \eta_{e,j}, \qquad\qquad\quad j = 1, \ldots, J, \quad e = 1, \ldots, E, \\
&\qquad\qquad -\eta_{e,j} \le A_{e,j} T_e s \le \eta_{e,j}, \quad j = 1, \ldots, J, \quad e = 1, \ldots, E, \\
&\qquad\qquad -\alpha\mathbf{1} \le \zeta \le \alpha\mathbf{1},
\end{aligned}
\tag{19}
$$

which is an LP problem in variables λ, s, ζ, and η. Let $(\bar{\lambda}, \bar{s}, \bar{\zeta}, \bar{\eta})$ denote the optimal solution of (19). The opportune-case load, defined as the optimal solution of problem (17), is then obtained straightforwardly as $\tilde{p} + Q\bar{\zeta}$. In short, $\lambda_{\max}(\alpha, \tilde{p})$ and the corresponding load can be obtained by solving LP problem (19).

Remark 3.3. In this paper we assume that only the fixed load, p, is uncertain and that the reference load, f, is known precisely. Introducing uncertainties in f might require more careful consideration. The worst case is characterized as the case with the minimum value of the limit load factor, and f is multiplied by the load factor. Therefore, if we allow that the norm of f can change due to uncertainty, then it affects the limit load factor. For instance, suppose that f is proportionally increased as βf

($\beta > 1$). Then the limit load factor is multiplied by $1/\beta$, i.e., it is decreased. From a physical point of view, however, this does not mean that load βf is worse than load f; the collapse loads in these two cases are the same. This observation may suggest that, when we consider uncertainty in f, the loads included in the uncertainty set should be normalized in some manner. The method of normalization suitable for worst-case analysis may possibly be nontrivial and an interesting subject of study. This issue, however, is not pursued further in this paper.

3B. *MILP formulation.* In Section 3A we defined the worst-case limit load factor by (15). The uncertainty model of p has been given by (14). The following proposition presents a nonlinear programming formulation of the worst scenario problem.

Proposition 3.4. *The worst-case limit load factor, $\lambda_{\min}(\alpha, \tilde{p})$, is equal to the optimal value of the following optimization problem*:

$$\text{Minimize } -\alpha \| Q^{\mathrm{T}} u \|_1 - \tilde{p}^{\mathrm{T}} u + \sum_{e=1}^{E} \sum_{j=1}^{J} R_{e,j} \gamma_{e,j} \text{ over } u, \gamma, z$$

$$\text{subject to} \quad f^{\mathrm{T}} u = 1,$$

$$\sum_{e=1}^{E} \sum_{j=1}^{J} (A_{e,j} T_e)^{\mathrm{T}} z_{e,j} = H^{\mathrm{T}} u, \tag{20}$$

$$\gamma_{e,j} \geq \| z_{e,j} \|_\infty, \quad e = 1, \ldots, E, \ j = 1, \ldots, J.$$

Here u, γ, and z are variables to be optimized.

A proof of Proposition 3.4 appears in Section A.2.

Let $(\bar{u}, \bar{\gamma}, \bar{z})$ be an optimal solution of problem (20). Here $\bar{u}$ is the collapse mode corresponding to the worst-case load. The worst-case load itself is obtained from $\bar{u}$ as follows. As shown in the proof of Proposition 3.4 (see (42)), $\bar{\zeta}$ satisfies

$$\bar{\zeta} \in \arg\min_{\zeta} \{ -(Q^{\mathrm{T}} \bar{u})^{\mathrm{T}} \zeta \mid \alpha \geq \| \zeta \|_\infty \}. \tag{21}$$

This is an LP problem in terms of ζ and its optimal solution is given by

$$\bar{\zeta}_l \in \begin{cases} \{\alpha\} & \text{if } q_l^{\mathrm{T}} \bar{u} > 0, \\ [-\alpha, \alpha] & \text{if } q_l^{\mathrm{T}} \bar{u} = 0, \\ \{-\alpha\} & \text{if } q_l^{\mathrm{T}} \bar{u} < 0. \end{cases} \tag{22}$$

Here $q_1, \ldots, q_L \in \mathbb{R}^d$ are column vectors of Q, i.e.,

$$Q = \left[q_1 \,\middle|\, q_2 \,\middle|\, \cdots \,\middle|\, q_L \right].$$

Accordingly, from definition (13) of p, the worst-case load, denoted $\bar{p}$, is obtained as

$$\bar{p} = \tilde{p} + Q\bar{\zeta}.$$

Problem (20) is a nonconvex optimization problem, because $-\alpha \| Q^{\mathrm{T}} u \|_1$ is a nonconvex function of u. This problem should be solved by an algorithm with guaranteed global convergence, because, obviously,

a local (but not global) optimal solution is not the worst scenario. Unfortunately, it is difficult to solve problem (20) globally due to its nonconvexity. This difficulty motivates the following proposition, which converts problem (20) to an MILP problem.

Proposition 3.5. *The optimal solution of problem* (20) *is also optimal for the following optimization problem*:

$$\text{Minimize} \quad -\alpha \sum_{l=1}^{L} w_l - \tilde{\boldsymbol{p}}^{\mathrm{T}} \boldsymbol{u} + \sum_{e=1}^{E} \sum_{j=1}^{J} R_{e,j} \gamma_{e,j} \quad \text{over } \boldsymbol{t}, \boldsymbol{u}, \boldsymbol{\gamma}, \boldsymbol{z}, \boldsymbol{w}$$

$$\text{subject to} \quad \boldsymbol{f}^{\mathrm{T}} \boldsymbol{u} = 1,$$

$$\sum_{e=1}^{E} \sum_{j=1}^{J} (\boldsymbol{A}_{e,j} \boldsymbol{T}_e)^{\mathrm{T}} z_{e,j} = \boldsymbol{H}^{\mathrm{T}} \boldsymbol{u}, \tag{23}$$

$$\gamma_{e,j} \geq \|z_{e,j}\|_{\infty}, \quad e = 1, \dots, E, \ j = 1, \dots, J,$$

$$\boldsymbol{w} \leq \boldsymbol{Q}^{\mathrm{T}} \boldsymbol{u} + M\boldsymbol{t},$$

$$\boldsymbol{w} \leq -\boldsymbol{Q}^{\mathrm{T}} \boldsymbol{u} + M(\boldsymbol{1} - \boldsymbol{t}),$$

$$\boldsymbol{t} \in \{0, 1\}^{L},$$

where $M \gg 0$ is a sufficiently large constant.

A proof of Proposition 3.5 appears in Section A.3. In problem (23), $\boldsymbol{w}$ and $\boldsymbol{t}$ are additional variables used for reformulation. At an optimal solution, these variables are related to the collapse mode, $\bar{\boldsymbol{u}}$, as

$$\bar{w}_l = |\boldsymbol{q}_l^{\mathrm{T}} \bar{\boldsymbol{u}}|, \quad \bar{t}_l \in \begin{cases} \{0\} & \text{if } \boldsymbol{q}_l^{\mathrm{T}} \bar{\boldsymbol{u}} > 0, \\ \{0, 1\} & \text{if } \boldsymbol{q}_l^{\mathrm{T}} \bar{\boldsymbol{u}} = 0, \\ \{1\} & \text{if } \boldsymbol{q}_l^{\mathrm{T}} \bar{\boldsymbol{u}} < 0. \end{cases} \tag{24}$$

Problem (23) is an MILP problem, because all the constraints other than the integrality constraints on $\boldsymbol{t}$ are linear constraints and the objective function is a linear function. Therefore, it can be solved by using an algorithm with guaranteed convergence to a global optimal solution. A branch-and-cut method is an example of such algorithms [Wolsey 1998; Aardal et al. 2005]. Moreover, several well-developed software packages, e.g., Gurobi Optimizer [Gurobi 2013] and CPLEX [IBM ILOG 2011], are available for solving this optimization problem.

3C. *Another uncertainty set.* In Sections 3A and 3B we assumed that the uncertainty of the external load, $\boldsymbol{p}$, is defined by (14). Instead of the ℓ^{∞}-norm used in (14), this section addresses an uncertain model defined by using the ℓ^1-norm, that is,

$$P(\alpha) = \{\tilde{\boldsymbol{p}} + \boldsymbol{Q}\boldsymbol{\zeta} \mid \|\boldsymbol{\zeta}\|_1 \leq \alpha\}. \tag{25}$$

In (14), the components of $\boldsymbol{\zeta}$ can perturb independently; for instance, when $\zeta_i = \alpha$, $\zeta_j \ (j \neq i)$ can take any value in $[-\alpha, \alpha]$. In contrast, (25) takes into account some sort of correlation; for instance, $\zeta_i = \alpha$ implies $\zeta_j = 0 \ (j \neq i)$. In other words, (14) is somewhat more pessimistic (or more conservative) than (25). In the following we show that uncertainty set (25) also allows MILP reformulation of the worst scenario detection problem.

The worst scenario detection problem is defined by (15) with (25). Analogous to Proposition 3.4, we can show that this problem is converted to the following nonlinear programming problem:

$$\text{Minimize} \quad -\alpha \| \boldsymbol{Q}^{\mathrm{T}} \boldsymbol{u} \|_{\infty} - \tilde{\boldsymbol{p}}^{\mathrm{T}} \boldsymbol{u} + \sum_{e=1}^{E} \sum_{j=1}^{J} R_{e,j} \gamma_{e,j} \quad \text{over } \boldsymbol{u}, \boldsymbol{\gamma}, \boldsymbol{z}$$

$$\text{subject to} \quad \boldsymbol{f}^{\mathrm{T}} \boldsymbol{u} = 1,$$

$$\sum_{e=1}^{E} \sum_{j=1}^{J} (\boldsymbol{A}_{e,j} \boldsymbol{T}_e)^{\mathrm{T}} \boldsymbol{z}_{e,j} = \boldsymbol{H}^{\mathrm{T}} \boldsymbol{u}, \tag{26}$$

$$\gamma_{e,j} \geq \| \boldsymbol{z}_{e,j} \|_{\infty}, \quad e = 1, \ldots, E, \ j = 1, \ldots, J.$$

Compared with problem (20), nonconvex term $-\alpha \| \boldsymbol{Q}^{\mathrm{T}} \boldsymbol{u} \|_1$ in the objective function is replaced by $-\alpha \| \boldsymbol{Q}^{\mathrm{T}} \boldsymbol{u} \|_{\infty}$. This is because the ℓ^1-norm (in (25)) is the dual norm of the ℓ^{∞}-norm (in (14)).

In a manner similar to Proposition 3.5, problem (26) also can be reformulated as an MILP problem. The result is formally stated as follows.

Proposition 3.6. *The optimal solution of problem* (26) *is also optimal for the following optimization problem*:

$$\text{Minimize} \quad -\alpha v - \tilde{\boldsymbol{p}}^{\mathrm{T}} \boldsymbol{u} + \sum_{e=1}^{E} \sum_{j=1}^{J} R_{e,j} \gamma_{e,j} \quad \text{over } \boldsymbol{t}, \boldsymbol{y}, \boldsymbol{u}, \boldsymbol{\gamma}, \boldsymbol{z}, \boldsymbol{w}, v$$

$$\text{subject to} \quad \boldsymbol{f}^{\mathrm{T}} \boldsymbol{u} = 1,$$

$$\sum_{e=1}^{E} \sum_{j=1}^{J} (\boldsymbol{A}_{e,j} \boldsymbol{T}_e)^{\mathrm{T}} \boldsymbol{z}_{e,j} = \boldsymbol{H}^{\mathrm{T}} \boldsymbol{u},$$

$$\gamma_{e,j} \geq \| \boldsymbol{z}_{e,j} \|_{\infty}, \qquad e = 1, \ldots, E, \ j = 1, \ldots, J,$$

$$\boldsymbol{w} \leq \boldsymbol{Q}^{\mathrm{T}} \boldsymbol{u} + M \boldsymbol{t}, \tag{27}$$

$$\boldsymbol{w} \leq -\boldsymbol{Q}^{\mathrm{T}} \boldsymbol{u} + M (\boldsymbol{1} - \boldsymbol{t}),$$

$$v \leq w_l + M (1 - y_l), \qquad l = 1, \ldots, L,$$

$$\sum_{l=1}^{L} y_l = 1,$$

$$\boldsymbol{t} \in \{0, 1\}^L, \quad \boldsymbol{y} \in \{0, 1\}^L.$$

A proof of Proposition 3.6 is slightly more complicated than one for Proposition 3.5; see Section A.4.

Let $(\bar{\boldsymbol{t}}, \bar{\boldsymbol{y}}, \bar{\boldsymbol{u}}, \bar{\boldsymbol{\gamma}}, \bar{\boldsymbol{z}}, \bar{\boldsymbol{w}}, \bar{v})$ denote the optimal solution of problem (27). Auxiliary variables, $\bar{w}_l$ and $\bar{t}_l$, are related to $\bar{\boldsymbol{u}}$ by (24). Moreover, $\bar{v}$ and $\bar{\boldsymbol{w}}$ satisfy $\bar{v} = \max\{\bar{w}_1, \ldots, \bar{w}_L\}$ and $\bar{y}_l = 1$ implies $\bar{v} = \bar{w}_l$.

4. Numerical experiments

The worst loading scenarios of two planar frame structures were found by solving MILP problem (23). Computation was carried out on a Core i5 (2.6 GHz) processor with 8.0 GB RAM. The data of the MILP

problems were prepared in the CPLEX LP file format [IBM ILOG 2011] with MATLAB 7.13. Then the MILP problems were solved with CPLEX Version 12.4 under the parameter setting "aggressive cuts".

4A. *Eccentrically braced five-story frame.* Consider the five-story plane frame in Figure 3. The nominal load, $\tilde{p}$, is defined as vertical point forces as shown in Figure 3, where $\tilde{p}_a = 180\,\text{kN}$ and $\tilde{p}_b = 90\,\text{kN}$. The proportionally increasing load, λf, is given as horizontal forces (in kN) as shown in Figure 3. The frame consists of $E = 65$ beam elements and $d = 120$ degrees of freedom, where each of the long beams is divided into two Euler–Bernoulli beam elements.

We adopt the following steel sections:

- A beam has cross-sectional area $7,000\,\text{mm}^2$ and plastic section modulus $850,000\,\text{mm}^3$, which approximately corresponds to an H-section with depth 294 mm, width 200 mm, web thickness 8 mm, and flange thickness 12 mm.

- A column has cross-sectional area $10,000\,\text{mm}^2$ and plastic section modulus $1,150,000\,\text{mm}^3$, which approximately corresponds to a square hollow section with edge length 300 mm and thickness 9 mm.

- A brace has cross-sectional area $10,000\,\text{mm}^2$ and plastic section modulus $825,000\,\text{mm}^3$, which approximately corresponds to a circular hollow section with external diameter 267.4 mm and thickness 12.7 mm.

The yield condition is defined by (4) with $\kappa = 0.85\sqrt{2}$. Here q_e^y and m_e^y are defined by $q_e^y = \sigma^y a_e$ and $m_e^y = \sigma^y Z_e^p$, where a_e and Z_e^p denote the cross-sectional area and the plastic section modulus, respectively, and $\sigma^y = 300\,\text{N/mm}^2$ is the material yield strength.

The nominal limit load factor of the frame is $\bar{\lambda}(\tilde{p}) = \lambda_{\min}(0) = 1126.5710$. The uncertainty model of p is defined by (14). The coefficient matrix Q is defined so that uncertain horizontal and vertical forces within the range $[-\alpha, \alpha]$ (in kN) possibly present at the nodes subjected to $\tilde{p}_a$. However, at the leftmost nodes only vertical forces are considered uncertain, because horizontal proportionally increasing forces are applied to these nodes. We suppose that no external moments are applied. Then Q results in a 120×55 matrix, the components of which are either 0 or 1 kN. For a given level of uncertainty $\alpha > 0$, the worst-case limit load factor, $\lambda_{\min}(\alpha)$, is computed by solving problem (23).
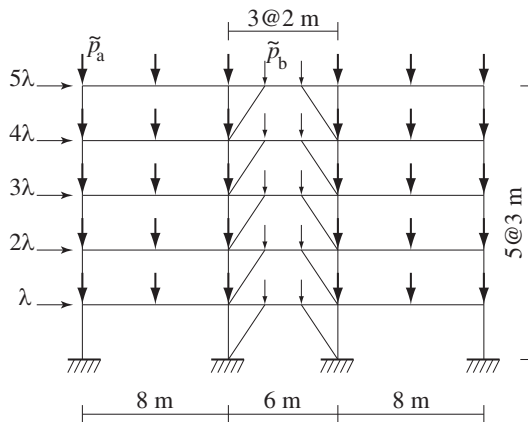

**Figure 3.** A five-story braced frame.
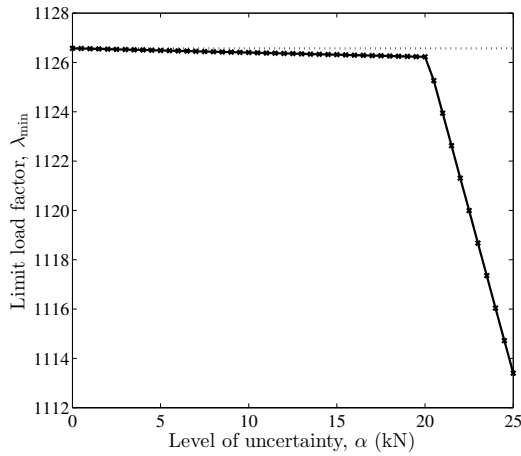
Figure 4. The variation of $\lambda_{\min}$ for the five-story frame.

The variation of $\lambda_{\min}(\alpha)$ with respect to α is depicted as a solid line in Figure 4. The dotted line shows the variation of the maximum limit load factor, $\lambda_{\max}(\alpha)$, which was obtained by solving problem (19). In this example, $\lambda_{\max}(\alpha)$ is constant within the range $0 \leq \alpha \leq 25$ kN. Concerning the worst-case limit load factor, at $\alpha = 18$ and 25 kN we obtain $\lambda_{\min}(18) = 1126.2593$ and $\lambda_{\min}(25) = 1113.3987$. CPLEX needed 7.4 s and 3.5 s to solve these two problems. Figure 5 depicts the collapse modes in the worst

$\alpha = 0$ kN $\alpha = 18$ kN $\alpha = 25$ kN
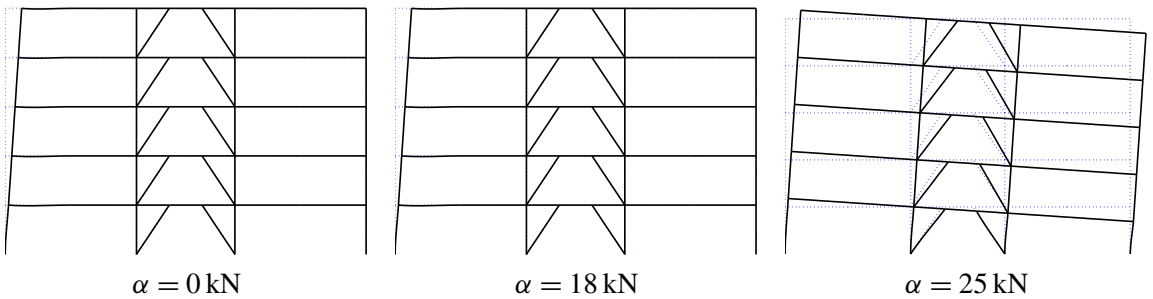
Figure 5. The collapse modes of the five-story frame, for various values of α.

$\alpha = 18$ kN $\alpha = 25$ kN
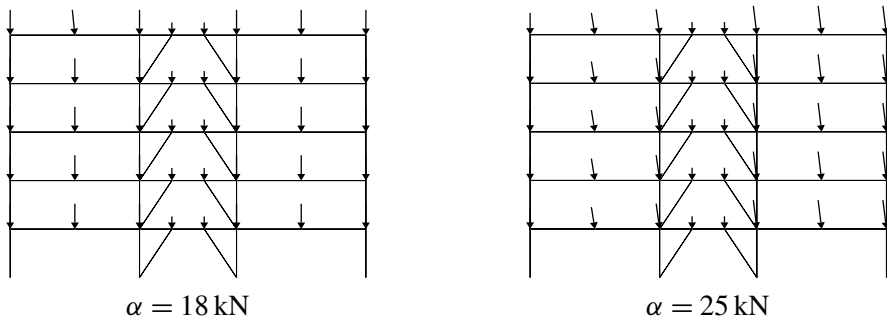
Figure 6. The worst-case loads for the five-story frame.

cases for $\alpha = 0$, 18, and 25 kN. It is observed that the collapse mode at $\alpha = 18$ kN is the same as that at $\alpha = 0$, while the collapse mode at $\alpha = 25$ kN is very different. Figure 6 shows the worst-case loads for $\alpha = 18$ kN and $\alpha = 25$ kN. Here the worst-case load is obtained using (22), choosing $\bar{\zeta}_l = 0$ for l satisfying $\boldsymbol{q}_l^{\mathrm{T}} \bar{\boldsymbol{u}} = 0$. In accordance with the difference of collapse modes, the worst-case loads of these two cases are also different.

4B. *Seven-story portal frame.* We next consider the seven-story plane frame in Figure 7. The nominal load, $\tilde{\boldsymbol{p}}$, is defined as vertical point forces with $\tilde{p}_a = 3000$ kN. The proportionally increasing load, $\lambda \boldsymbol{f}$, is given as horizontal forces λ kN applied at the leftmost nodes. The frame consists of $E = 49$ beam elements and $d = 105$ degrees of freedom, where each beam is divided into two beam elements.

We use the following steel sections:

- A beam on the lower three stories has cross-sectional area 5,000 mm² and plastic section modulus 370,000 mm³, which approximately corresponds to an H-section with depth 175 mm, width 175 mm, web thickness 7.5 mm, and flange thickness 11 mm.

- A beam on the upper stories has cross-sectional area 2,000 mm² and plastic section modulus 90,000 mm³, which approximately corresponds to an H-section with depth 100 mm, width 100 mm, web thickness 6 mm, and flange thickness 8 mm.

- A column on the lower three stories has cross-sectional area 24,000 mm² and plastic section modulus 2,970,000 mm³, which approximately corresponds to a square hollow section with edge length 350 mm and thickness 19 mm.

- A column on the upper stories has cross-sectional area 13,000 mm² and plastic section modulus 1,440,000 mm³, which approximately corresponds to a square hollow section with edge length 300 mm and thickness 12 mm.

The yield condition is defined by (4) with $\kappa = 0.85\sqrt{2}$ and $\sigma^y = 300$ N/mm² in the same manner as in Section 4A.
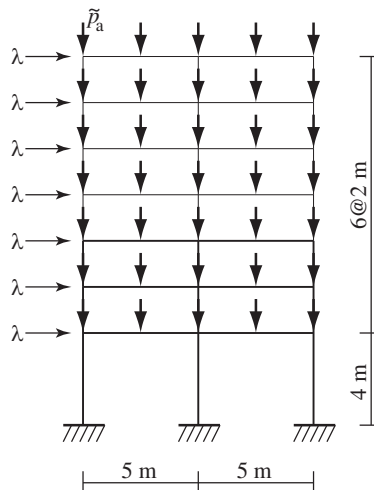
Figure 7. A seven-story portal frame.
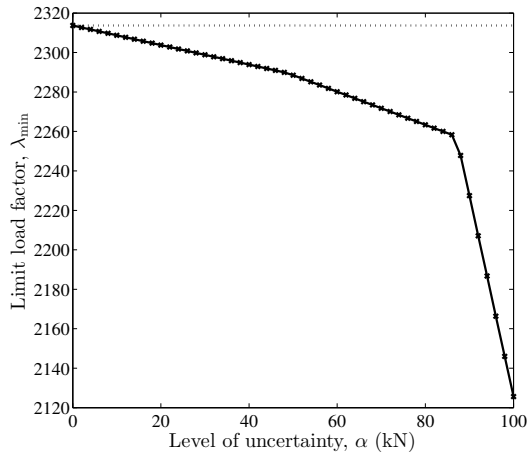
Figure 8. The variation of $\lambda_{\min}$ for the seven-story frame.

The nominal limit load factor of the frame is $\bar{\lambda}(\tilde{p}) = \lambda_{\min}(0) = 2313.6687$. The uncertainty model of p is defined by (14). The coefficient matrix Q is defined so that uncertain horizontal and vertical forces within the range $[-\alpha, \alpha]$ (in kN) possibly present at the nodes. However, at the leftmost nodes only vertical forces are considered uncertain. Then Q results in a 105×63 matrix.

The solid line in Figure 8 shows the variation of the worst-case limit load factor, $\lambda_{\min}(\alpha)$, with respect to α. The dotted line shows the variation of the maximum limit load factor, $\lambda_{\max}(\alpha)$, which is constant within the range $0 \leq \alpha \leq 100$ kN. Concerning the worst-case limit load factor, at $\alpha = 20, 80$, and 100 kN we obtain $\lambda_{\min}(20) = 2303.7830$, $\lambda_{\min}(80) = 2263.3615$, and $\lambda_{\min}(100) = 2125.5923$. CPLEX needed 0.8 s, 4.0 s, and 10.4 s, respectively, to solve these three problems. Figure 9 collects the collapse modes in the worst scenarios obtained . The mode at $\alpha = 20$ kN is the same as that in the nominal case ($\alpha = 0$). However, the modes at $\alpha = 80$ kN and $\alpha = 100$ kN are different from that in the nominal case. Thus the collapse mode in the most severe scenario depends on the level of uncertainty, α. The worst-case loads, p_w, are shown in Figure 10. It may be observed in Figure 8 that the graph of $\lambda_{\min}(\alpha)$ has two angular
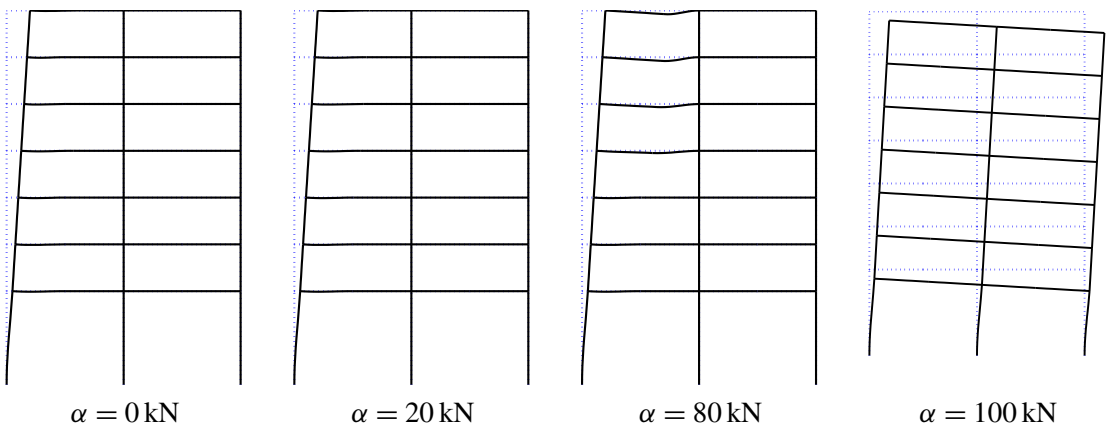
Figure 9. The collapse modes of the seven-story frame.

$\alpha = 20 \, \text{kN}$ $\alpha = 80 \, \text{kN}$ $\alpha = 100 \, \text{kN}$
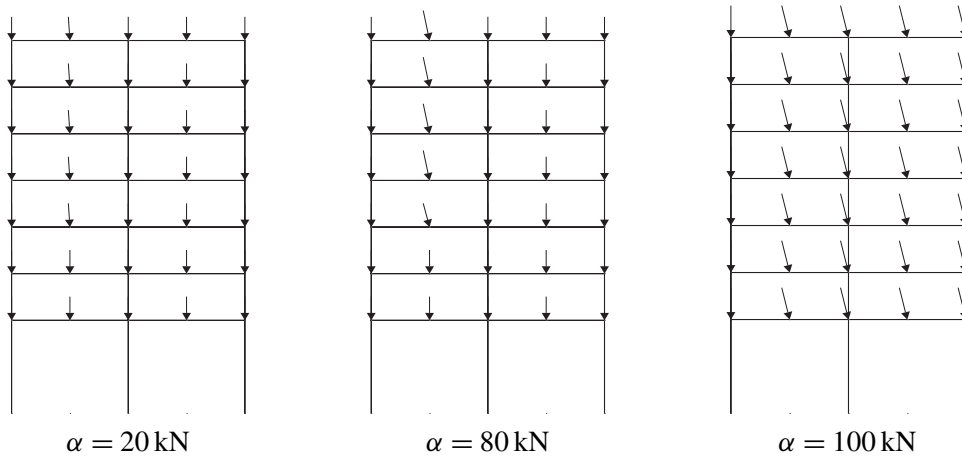
Figure 10. The worst-case loads for the seven-story frame.

points. Similarly, the curve in Figure 4 has one angular point. It seems that these sudden changes of the slope of the curve are due to changes of the collapse modes corresponding to $\lambda_{\min}(\alpha)$.

5. Conclusions

Evaluating robustness against uncertainty is a key to many design methodologies of structures. In some engineering problems including severe uncertainty, e.g., uncertainty in large earthquakes [Takewaki et al. 2013], knowledge of uncertain parameters is fundamentally limited and reliable stochastic data on uncertain parameters is unavailable. Nonprobabilistic uncertainty analysis, rather than probabilistic, might be applicable in grasping the critical response of a structure to estimate the safety level. This paper has developed a solid numerical method for finding the worst-case load at which the plastic limit load factor of a given frame structure attains the worst value.

Finding the worst scenario among a given set of possible scenarios is formulated in general as an optimization problem. In this paper this worst scenario problem has been converted to a mixed-integer linear programming (MILP) problem. Several well-developed software packages are available for finding a global optimal solution of an MILP problem. Guaranteed convergence to a global optimal solution warrants that the proposed method provides the precisely worst response of the structure; that is, neither overestimate nor underestimate arises. In addition, algorithms specifically designed for uncertainty analysis are not required. Also, implementation of optimization algorithms is not necessary.

This paper has assumed that yield conditions are represented as piecewise linear functions in terms of generalized stresses. Moreover, the uncertainty set of external loads has been restricted to polyhedra with specific forms. Extensions to curved yield surfaces and/or more general uncertainty sets remain to be explored. Also, extensions to shakedown analysis, possibly taking into account work-hardening effects [Maier 1970; Polizzotto et al. 1991] and dynamic loads [Corradi and Maier 1973–1974; Polizzotto et al. 1993], could be made. In the numerical examples it has been shown that the collapse mode in the worst case can possibly depend on the level of uncertainty in the external load. Numerical analysis using

more realistic structural designs could be performed for in-depth study of the influence of uncertainty on real-world structures.

Appendix: Proofs

A.1 *Derivation of dual limit analysis problem.* This section shows that problem (12) is derived as the Fenchel dual problem of problem (7).

For notational convenience, suppose that $A_{1,1}, \ldots, A_{E,J}$ are all $a \times 3$ matrices. Define vectors x and y by

$$
x = \begin{bmatrix} \lambda \\ s \end{bmatrix}, \quad
y = \begin{bmatrix} y^{\mathrm{a}} \\ \hline y^{\mathrm{b}} \\ \hline y^{\mathrm{c}}_{1,1} \\ \vdots \\ y^{\mathrm{c}}_{E,J} \end{bmatrix},
$$

with $\lambda \in \mathbb{R}$, $s \in \mathbb{R}^{3E}$, $y^{\mathrm{a}} \in \mathbb{R}^d$, $y^{\mathrm{b}} \in \mathbb{R}^{EJ}$, and $y^{\mathrm{c}}_{e,j} \in \mathbb{R}^a$ for all e and j. We write

$$
X = \mathbb{R} \times \mathbb{R}^{3E}, \quad Y = \mathbb{R}^d \times \mathbb{R}^{EJ} \times \mathbb{R}^{aEJ},
$$

for simplicity, where $x \in X$ and $y \in Y$. Define functions $f : X \to \mathbb{R}$ and $g : Y \to \mathbb{R} \cup \{+\infty\}$ by

$$
f(x) = -\lambda, \tag{28}
$$

$$
g(y) = \begin{cases} 0 & \text{if } y^{\mathrm{a}} = p, \ y^{\mathrm{b}}_{e,j} + R_{e,j} \geq \|y^{\mathrm{c}}_{e,j}\|_1 \ \text{ for all } e \text{ and } j, \\ +\infty & \text{otherwise}, \end{cases} \tag{29}
$$

which are proper convex functions. Define a matrix Λ by

$$
\Lambda = \begin{bmatrix} -f & H \\ \hline 0 & O \\ \hline 0 & -A_{1,1}T_1 \\ \vdots & \vdots \\ 0 & -A_{E,J}T_E \end{bmatrix}. \tag{30}
$$

With this setting, problem (7) is equivalently rewritten as

$$
\max\{-f(x) - g(\Lambda x) \mid x \in X\}. \tag{31}
$$

From standard results in Fenchel duality theory [Rockafellar 1970], the Fenchel dual problem of (31) is given by

$$
\min\{f^*(\Lambda^{\mathrm{T}} y^*) + g^*(-y^*) \mid y^* \in Y\}. \tag{32}
$$

Here $f^* : X \to \mathbb{R}$ and $g^* : Y \to \mathbb{R} \cup \{\infty\}$ are conjugate functions of f and g, respectively, and

$$
y^* = \begin{bmatrix} y^{a*} \\ \hline y^{b*} \\ \hline y^{c*}_{1,1} \\ \vdots \\ y^{c*}_{E,J} \end{bmatrix}.
$$

In the following we show that problem (32) with f, g, and Λ defined by (28), (29), and (30) is equivalent to problem (12).

With the notation $x^* = (\lambda^*, s^*) \in X$, f^* is explicitly written as

$$
\begin{aligned}
f^*(x^*) &= \sup\{\langle x, x^* \rangle - f(x) \mid x \in V\} \\
&= \sup_\lambda \{\lambda(\lambda^* + 1)\} + \sup_s \{s^{\mathrm{T}} s^*\} \\
&= \begin{cases} 0 & \text{if } \lambda^* = -1 \text{ and } s^* = \mathbf{0}, \\ +\infty & \text{otherwise.} \end{cases}
\end{aligned}
\tag{33}
$$

The conjugate function of g in (29) is obtained as follows. For notational convenience, define $K \subseteq \mathbb{R}^{a+1}$ by

$$
K = \{(r_0, r_1) \in \mathbb{R} \times \mathbb{R}^a \mid r_0 \ge \|r_1\|_1\}.
$$

By the definition of a conjugate function, we obtain

$$
g^*(y^*) = \sup\{\langle y, y^* \rangle \mid y \in \operatorname{dom} g\}
$$

$$
= \sup_{y^a}\{(y^a)^{\mathrm{T}} y^{a*} \mid y^a = p\} + \sup_{y^b, y^c} \sum_{e=1}^{E} \sum_{j=1}^{J} \left\{ \begin{bmatrix} y^b_{e,j} \\ y^c_{e,j} \end{bmatrix}^{\mathrm{T}} \begin{bmatrix} y^{b*}_{e,j} \\ y^{c*}_{e,j} \end{bmatrix} \middle| \begin{bmatrix} y^b_{e,j} + R_{e,j} \\ y^c_{e,j} \end{bmatrix} \in K \right\}
\tag{34}
$$

$$
= p^{\mathrm{T}} y^{a*} - \sum_{e=1}^{E} \sum_{j=1}^{J} R_{e,j} y^{b*}_{e,j} + \sum_{e=1}^{E} \sum_{j=1}^{J} \sup_{y^b_{e,j}, y^c_{e,j}} \left\{ \begin{bmatrix} y^b_{e,j} + R_{e,j} \\ y^c_{e,j} \end{bmatrix}^{\mathrm{T}} \begin{bmatrix} y^{b*}_{e,j} \\ y^{c*}_{e,j} \end{bmatrix} \middle| \begin{bmatrix} y^b_{e,j} + R_{e,j} \\ y^c_{e,j} \end{bmatrix} \in K \right\}.
$$

Since the dual cone of K is given by (see, for example, [Boyd and Vandenberghe 2004, Example 2.25])

$$
K^* = \{(r_0^*, r_1^*) \in \mathbb{R} \times \mathbb{R}^a \mid r_0^* \ge \|r_1^*\|_\infty\},
$$

we have that

$$
\sup_{r_0, r_1} \left\{ \begin{bmatrix} r_0 \\ r_1 \end{bmatrix}^{\mathrm{T}} \begin{bmatrix} r_0^* \\ r_1^* \end{bmatrix} \middle| \begin{bmatrix} r_0 \\ r_1 \end{bmatrix} \in K \right\} = \begin{cases} 0 & \text{if } - \begin{bmatrix} r_0^* \\ r_1^* \end{bmatrix} \in K^*, \\ +\infty & \text{otherwise.} \end{cases}
$$

With this observation we see that (34) is reduced to

$$
g^*(y^*) = \begin{cases} p^{\mathrm{T}} y^{a*} - \sum_{e=1}^{E} \sum_{j=1}^{J} R_{e,j} y^{b*}_{e,j} & \text{if } - y^{b*}_{e,j} \ge \|-y^{c*}_{e,j}\|_\infty \text{ for all } e \text{ and } j, \\ +\infty & \text{otherwise.} \end{cases}
\tag{35}
$$

From definition (30) of $\boldsymbol{\Lambda}$, $\boldsymbol{\Lambda}^{\mathrm{T}} \boldsymbol{y}^*$ is written as

$$\boldsymbol{\Lambda}^{\mathrm{T}} \boldsymbol{y}^* = \begin{bmatrix} -\boldsymbol{f}^{\mathrm{T}} \boldsymbol{y}^{\mathrm{a}*} \\ \boldsymbol{H}^{\mathrm{T}} \boldsymbol{y}^{\mathrm{a}*} - \sum_{e=1}^{E} \sum_{j=1}^{J} (\boldsymbol{A}_{e,j} \boldsymbol{T}_e)^{\mathrm{T}} \boldsymbol{y}_{e,j}^{\mathrm{c}*} \end{bmatrix}. \tag{36}$$

By using (33), (35), and (36), we obtain

$$f^*(\boldsymbol{\Lambda}^{\mathrm{T}} \boldsymbol{y}^*) = \begin{cases} 0 & \text{if } -\boldsymbol{f}^{\mathrm{T}} \boldsymbol{y}^{\mathrm{a}*} = -1, \ \boldsymbol{H}^{\mathrm{T}} \boldsymbol{y}^{\mathrm{a}*} - \sum_{e=1}^{E} \sum_{j=1}^{J} (\boldsymbol{A}_{e,j} \boldsymbol{T}_e)^{\mathrm{T}} \boldsymbol{y}_{e,j}^{\mathrm{c}*} = \boldsymbol{0}, \\ +\infty & \text{otherwise}, \end{cases} \tag{37}$$

$$g^*(-\boldsymbol{y}^*) = \begin{cases} -\boldsymbol{p}^{\mathrm{T}} \boldsymbol{y}^{\mathrm{a}*} + \sum_{e=1}^{E} \sum_{j=1}^{J} R_{e,j} y_{e,j}^{\mathrm{b}*} & \text{if } y_{e,j}^{\mathrm{b}*} \geq \|\boldsymbol{y}_{e,j}^{\mathrm{c}*}\|_{\infty} \text{ for all } e \text{ and } j, \\ +\infty & \text{otherwise}. \end{cases} \tag{38}$$

From (37) and (38), the Fenchel dual problem in (32) is explicitly written as

$$\begin{aligned}
\text{Minimize } & -\boldsymbol{p}^{\mathrm{T}} \boldsymbol{y}^{\mathrm{a}*} + \sum_{e=1}^{E} \sum_{j=1}^{J} R_{e,j} y_{e,j}^{\mathrm{b}*} \\
\text{subject to } & \boldsymbol{f}^{\mathrm{T}} \boldsymbol{y}^{\mathrm{a}*} = 1, \\
& \sum_{e=1}^{E} \sum_{j=1}^{J} (\boldsymbol{A}_{e,j} \boldsymbol{T}_e)^{\mathrm{T}} \boldsymbol{y}_{e,j}^{\mathrm{c}*} = \boldsymbol{H}^{\mathrm{T}} \boldsymbol{y}^{\mathrm{a}*}, \\
& y_{e,j}^{\mathrm{b}*} \geq \|\boldsymbol{y}_{e,j}^{\mathrm{c}*}\|_{\infty}, \quad e = 1, \dots, E, \ j = 1, \dots, J.
\end{aligned} \tag{39}$$

By rewriting the dual variables as

$$\boldsymbol{y}^{\mathrm{a}*} = \boldsymbol{u}, \quad \boldsymbol{y}^{\mathrm{b}*} = \boldsymbol{\gamma}, \quad \boldsymbol{y}^{\mathrm{c}*} = \boldsymbol{z},$$

we see that problem (39) indeed coincides with problem (12). Thus problem (12) is obtained as the Fenchel dual problem of (7).

Note that problems (7) and (12) can be converted to LP problems; see Remarks 2.3 and 2.4. As mentioned in Section 2B, we assume that problem (7) has an optimal solution. Then the duality theory of LP guarantees that problems (7) and (12) share the same optimal value.

A.2 *Proof of Proposition 3.4.* Since $\bar{\lambda}(\boldsymbol{p})$ is the optimal value of problem (12), (15) can be rewritten as

$$\lambda_{\min}(\alpha, \tilde{\boldsymbol{p}}) = \min_{\boldsymbol{p} \in P(\alpha, \tilde{\boldsymbol{p}})} \left\{ \min_{\boldsymbol{u}, \boldsymbol{\gamma}, \boldsymbol{z}} \left\{ -\boldsymbol{p}^{\mathrm{T}} \boldsymbol{u} + \sum_{e=1}^{E} \sum_{j=1}^{J} R_{e,j} \gamma_{e,j} \ \middle| \ (\boldsymbol{u}, \boldsymbol{\gamma}, \boldsymbol{z}) \in U \right\} \right\}, \tag{40}$$

where U is the feasible set of problem (12). By reversing the order of the two minimizations in (40), we obtain

$$\lambda_{\min}(\alpha, \tilde{\boldsymbol{p}}) = \min_{(\boldsymbol{u}, \boldsymbol{\gamma}, \boldsymbol{z}) \in U} \left\{ \min_{\boldsymbol{p}} \left\{ -\boldsymbol{p}^{\mathrm{T}} \boldsymbol{u} \ \middle| \ \boldsymbol{p} \in P(\alpha, \tilde{\boldsymbol{p}}) \right\} + \sum_{e=1}^{E} \sum_{j=1}^{J} R_{e,j} \gamma_{e,j} \right\}. \tag{41}$$

By using (14) and the Hölder inequality [Steele 2004, Chapter 9], the inner minimization problem of (41) can be reduced to

$$
\begin{aligned}
\min_{\boldsymbol{p}}\{-\boldsymbol{p}^{\mathrm{T}}\boldsymbol{u} \mid \boldsymbol{p} \in P(\alpha, \tilde{\boldsymbol{p}})\} &= \min_{\boldsymbol{\zeta}}\{-(\boldsymbol{Q}^{\mathrm{T}}\boldsymbol{u})^{\mathrm{T}}\boldsymbol{\zeta} \mid \alpha \geq \|\boldsymbol{\zeta}\|_{\infty}\} - \tilde{\boldsymbol{p}}^{\mathrm{T}}\boldsymbol{u} \\
&= \min_{\boldsymbol{\zeta}}\{-\|\boldsymbol{Q}^{\mathrm{T}}\boldsymbol{u}\|_{1}\|\boldsymbol{\zeta}\|_{\infty} \mid \alpha \geq \|\boldsymbol{\zeta}\|_{\infty}\} - \tilde{\boldsymbol{p}}^{\mathrm{T}}\boldsymbol{u} \\
&= -\alpha\|\boldsymbol{Q}^{\mathrm{T}}\boldsymbol{u}\|_{1} - \tilde{\boldsymbol{p}}^{\mathrm{T}}\boldsymbol{u}.
\end{aligned}
\tag{42}
$$

Here the last equality is actually attained by choosing $\boldsymbol{\zeta}$ as

$$
\zeta_l = \begin{cases} \alpha & \text{if } \boldsymbol{q}_l^{\mathrm{T}}\boldsymbol{u} > 0, \\ 0 & \text{if } \boldsymbol{q}_l^{\mathrm{T}}\boldsymbol{u} = 0, \\ -\alpha & \text{if } \boldsymbol{q}_l^{\mathrm{T}}\boldsymbol{u} < 0, \end{cases}
$$

where $\boldsymbol{q}_1, \ldots, \boldsymbol{q}_L \in \mathbb{R}^d$ are column vectors of $\boldsymbol{Q}$, i.e.,

$$
\boldsymbol{Q} = \begin{bmatrix} \boldsymbol{q}_1 \mid \boldsymbol{q}_2 \mid \cdots \mid \boldsymbol{q}_L \end{bmatrix}.
$$

Substitution of (42) into problem (41) results in problem (20).

A.3 *Proof of Proposition 3.5.* In the objective function of problem (20), only $-\alpha\|\boldsymbol{Q}^{\mathrm{T}}\boldsymbol{u}\|_{1}$ is a nonconvex term. This term is explicitly written as

$$
-\alpha\|\boldsymbol{Q}^{\mathrm{T}}\boldsymbol{u}\|_{1} = -\alpha \sum_{l=1}^{L} |\boldsymbol{q}_l^{\mathrm{T}}\boldsymbol{u}|,
\tag{43}
$$

where $\boldsymbol{q}_1, \ldots, \boldsymbol{q}_L \in \mathbb{R}^d$ are column vectors of $\boldsymbol{Q}$. For each $l = 1, \ldots, L$, let w_l be an additional variable that serves as a lower bound for $|\boldsymbol{q}_l^{\mathrm{T}}\boldsymbol{u}|$, i.e., $w_l \leq |\boldsymbol{q}_l^{\mathrm{T}}\boldsymbol{u}|$. Then minimizing (43) is equivalent to minimizing

$$
-\alpha \sum_{l=1}^{L} w_l
\tag{44}
$$

under the constraints

$$
(w_l \leq \boldsymbol{q}_l^{\mathrm{T}}\boldsymbol{u}) \vee (w_l \leq -\boldsymbol{q}_l^{\mathrm{T}}\boldsymbol{u}), \quad l = 1, \ldots, L.
\tag{45}
$$

Here $\vee$ denotes the logical "or". For each $l = 1, \ldots, L$, constraint (45) can be rewritten as

$$
\begin{aligned}
w_l &\leq \boldsymbol{q}_l^{\mathrm{T}}\boldsymbol{u} + M t_l, & \text{(46a)} \\
w_l &\leq -\boldsymbol{q}_l^{\mathrm{T}}\boldsymbol{u} + M(1 - t_l), & \text{(46b)} \\
t_l &\in \{0, 1\}, & \text{(46c)}
\end{aligned}
$$

where $M \gg 0$ is a sufficiently large constant. The upshot is that minimizing (43) is equivalent to minimizing (44) under constraint (46), and hence problem (20) is reduced to problem (23).

A.4 *Proof of Proposition 3.6.* In the objective function of problem (26), only the term

$$-\alpha \| \boldsymbol{Q}^{\mathrm{T}} \boldsymbol{u} \|_{\infty} = -\alpha \max\{|\boldsymbol{q}_l^{\mathrm{T}} \boldsymbol{u}| \mid l = 1, \ldots, L\} \tag{47}$$

is nonconvex. To rewrite this term we introduce additional variables w_l ($l = 1, \ldots, L$) and v, where w_l is a lower bound for $|\boldsymbol{q}_l^{\mathrm{T}} \boldsymbol{u}|$ and v is a lower bound for $\max\{w_1, \ldots, w_L\}$. Then minimizing (47) is equivalent to minimizing

$$-\alpha v \tag{48}$$

under the constraints

$$(v \le w_1) \vee \cdots \vee (v \le w_L), \tag{49a}$$

$$w_l \le |\boldsymbol{q}_l^{\mathrm{T}} \boldsymbol{u}|, \quad l = 1, \ldots, L, \tag{49b}$$

where $\vee$ denotes the logical "or". Furthermore, by introducing 0-1 variables $y_1, \ldots, y_L$, (49a) can be replaced with

$$v \le w_l + M(1 - y_l), \quad l = 1, \ldots, L, \tag{50a}$$

$$\sum_{l=1}^{L} y_l = 1, \tag{50b}$$

$$y_l \in \{0, 1\}, \qquad l = 1, \ldots, L, \tag{50c}$$

where $M \gg 0$ is a sufficiently large constant. Indeed, (50b) and (50c) imply that there exists unique $\hat{l} \in \{1, \ldots, L\}$ satisfying $y_{\hat{l}} = 1$ and $y_l = 0$ for all $l \ne \hat{l}$. Then (50a) reads

$$v \le w_{\hat{l}},$$

$$v \le w_l + M \text{ for all } l \ne \hat{l},$$

which allows $v > w_l$ for all $l \ne \hat{l}$. . Next, observe that (49b) can be rewritten as

$$(w_l \le \boldsymbol{q}_l^{\mathrm{T}} \boldsymbol{u}) \vee (w_l \le -\boldsymbol{q}_l^{\mathrm{T}} \boldsymbol{u}), \quad l = 1, \ldots, L. \tag{51}$$

By using 0-1 variables, (51) is rewritten as

$$w_l \le \boldsymbol{q}_l^{\mathrm{T}} \boldsymbol{u} + M t_l, \qquad l = 1, \ldots, L, \tag{52a}$$

$$w_l \le -\boldsymbol{q}_l^{\mathrm{T}} \boldsymbol{u} + M(1 - t_l), \quad l = 1, \ldots, L, \tag{52b}$$

$$t_l \in \{0, 1\}, \qquad l = 1, \ldots, L. \tag{52c}$$

As a consequence, we see that (49) is rewritten as (50) and (52). By using this, problem (26) is reduced to problem (27).

References

[Aardal et al. 2005] K. Aardal, G. L. Nemhauser, and R. Weismantel (editors), *Discrete optimization*, Handbooks in Operations Research and Management Science **12**, Elsevier, Amsterdam, 2005.

[Alefeld and Mayer 2000] G. Alefeld and G. Mayer, "Interval analysis: theory and applications", *J. Comput. Appl. Math.* **121**:1-2 (2000), 421–464.

[Alibrandi and Ricciardi 2008] U. Alibrandi and G. Ricciardi, "The use of stochastic stresses in the static approach of proba-
bilistic limit analysis", *Int. J. Numer. Methods Eng.* **73**:6 (2008), 747–782.

[Ben-Haim 2006] Y. Ben-Haim, *Information-gap decision theory: decisions under severe uncertainty*, 2nd ed., Academic
Press, San Diego, CA, 2006.

[Ben-Haim and Elishakoff 1990] Y. Ben-Haim and I. Elishakoff, *Convex models of uncertainty in applied mechanics*, Studies
in Applied Mechanics **25**, Elsevier, Amsterdam, 1990.

[Beyer and Sendhoff 2007] H.-G. Beyer and B. Sendhoff, "Robust optimization: a comprehensive survey", *Comput. Methods
Appl. Mech. Eng.* **196**:33-34 (2007), 3190–3218.

[Biondini et al. 2004] F. Biondini, F. Bontempi, and P. G. Malerba, "Fuzzy reliability analysis of concrete structures", *Comput.
Struct.* **82**:13–14 (2004), 1033–1052.

[Bjerager 1989] P. Bjerager, "Plastic systems reliability by LP and FORM", *Comput. Struct.* **31**:2 (1989), 187–196.

[Boyd and Vandenberghe 2004] S. Boyd and L. Vandenberghe, *Convex optimization*, Cambridge University Press, Cambridge,
2004.

[Caddemi et al. 2002] S. Caddemi, G. Ricciardi, and C. Saccà, "Limit analysis of structures with stochastic strengths by a static
approach", *Meccanica* **37**:6 (2002), 527–544.

[Catallo 2004] L. Catallo, "Genetic anti-optimization for reliability structural assessment of precast concrete structures", *Com-
put. Struct.* **82**:13-14 (2004), 1053–1065.

[Chen et al. 2002] S. Chen, H. Lian, and X. Yang, "Interval static displacement analysis for structures with interval parameters",
Int. J. Numer. Methods Eng. **53**:2 (2002), 393–407.

[Corradi and Maier 1973–1974] L. Corradi and G. Maier, "Inadaptation theorems in the dynamics of elastic work-hardening
structures", *Ing. Arch.* **43**:1 (1973–1974), 44–57.

[De Gersem et al. 2007] H. De Gersem, D. Moens, W. Desmet, and D. Vandepitte, "Interval and fuzzy dynamic analysis of
finite element models with superelements", *Comput. Struct.* **85**:5–6 (2007), 304–319.

[Degrauwe et al. 2010] D. Degrauwe, G. Lombaert, and G. De Roeck, "Improving interval analysis in finite element calcula-
tions by means of affine arithmetic", *Comput. Struct.* **88**:3–4 (2010), 247–254.

[Faigle et al. 2002] U. Faigle, W. Kern, and G. Still, *Algorithmic principles of mathematical programming*, Kluwer Texts in the
Mathematical Sciences **24**, Kluwer, Dordrecht, 2002.

[Guo et al. 2008] X. Guo, W. Bai, and W. Zhang, "Extreme structural response analysis of truss structures under material
uncertainty via linear mixed 0–1 programming", *Int. J. Numer. Methods Eng.* **76**:3 (2008), 253–277.

[Guo et al. 2009] X. Guo, W. Bai, and W. Zhang, "Confidence extremal structural response analysis of truss structures under
static load uncertainty via SDP relaxation", *Comput. Struct.* **87**:3–4 (2009), 246–253.

[Guo et al. 2011] X. Guo, J. Du, and X. Gao, "Confidence structural robust optimization by non-linear semidefinite programming-
based single-level formulation", *Int. J. Numer. Methods Eng.* **86**:8 (2011), 953–974.

[Gurobi 2013] *Gurobi optimizer reference manual*, Gurobi Optimization, Houston, TX, 2013, Available at http://www.gurobi.com.

[Hlaváček et al. 2004] I. Hlaváček, J. Chleboun, and I. Babuška, *Uncertain input data problems and the worst scenario method*,
North-Holland Series in Applied Mathematics and Mechanics **46**, Elsevier, Amsterdam, 2004.

[IBM ILOG 2011] *User's manual for CPLEX*, IBM ILOG, Armonk, NY, 2011, Available at http://www.ilog.com.

[Jung and Pulmano 1996] C. Y. Jung and V. A. Pulmano, "Improved fuzzy linear programming model for structure designs",
Comput. Struct. **58**:3 (1996), 471–477.

[Kanno 2012] Y. Kanno, "Worst scenario detection in limit analysis of trusses against deficiency of structural components",
Eng. Struct. **42** (2012), 33–42.

[Kanno and Takewaki 2006] Y. Kanno and I. Takewaki, "Confidence ellipsoids for static response of trusses with load and
structural uncertainties", *Comput. Methods Appl. Mech. Eng.* **196**:1-3 (2006), 393–403.

[Kanno and Takewaki 2007] Y. Kanno and I. Takewaki, "Worst case plastic limit analysis of trusses under uncertain loads via
mixed 0–1 programming", *J. Mech. Mater. Struct.* **2**:2 (2007), 245–273.

[Kanno and Takewaki 2008] Y. Kanno and I. Takewaki, "Semidefinite programming for uncertain linear equations in static analysis of structures", *Comput. Methods Appl. Mech. Eng.* **198**:1 (2008), 102–115.

[Kanno and Takewaki 2009] Y. Kanno and I. Takewaki, "Semidefinite programming for dynamic steady-state analysis of structures under uncertain harmonic loads", *Comput. Methods Appl. Mech. Eng.* **198**:41-44 (2009), 3239–3261.

[Langley 2000] R. S. Langley, "Unified approach to probabilistic and possibilistic analysis of uncertain systems", *J. Eng. Mech.* (*ASCE*) **126**:11 (2000), 1163–1172.

[Maier 1970] G. Maier, "A matrix structural theory of piecewise linear elastoplasticity with interacting yield planes", *Meccanica* **5**:1 (1970), 54–66.

[Marti 2008] K. Marti, "Limit load and shakedown analysis of plastic structures under stochastic uncertainty", *Comput. Methods Appl. Mech. Eng.* **198**:1 (2008), 42–51.

[Marti and Stoeckl 2004] K. Marti and G. Stoeckl, "Stochastic linear programming methods in limit load analysis and optimal plastic design under stochastic uncertainty", *Z. Angew. Math. Mech.* **84**:10–11 (2004), 666–677.

[McWilliam 2001] S. McWilliam, "Anti-optimization of uncertain structures using interval analysis", *Comput. Struct.* **79**:4 (2001), 421–430.

[Moens and Hanss 2011] D. Moens and M. Hanss, "Non-probabilistic finite element analysis for parametric uncertainty treatment in applied mechanics: recent advances", *Finite Elem. Anal. Des.* **47**:1 (2011), 4–16.

[Moens and Vandepitte 2005] D. Moens and D. Vandepitte, "A survey of non-probabilistic uncertainty treatment in finite element analysis", *Comput. Methods Appl. Mech. Eng.* **194**:12-16 (2005), 1527–1555.

[Möller and Beer 2008] B. Möller and M. Beer, "Engineering computation under uncertainty: capabilities of non-traditional models", *Comput. Struct.* **86**:10 (2008), 1024–1041.

[Munro and Chuang 1986] J. Munro and P.-H. Chuang, "Optimal plastic design with imprecise data", *J. Eng. Mech.* (*ASCE*) **112**:9 (1986), 888–903.

[Neumaier 1990] A. Neumaier, *Interval methods for systems of equations*, Encyclopedia of Mathematics and its Applications **37**, Cambridge University Press, 1990.

[Neumaier and Pownuk 2007] A. Neumaier and A. Pownuk, "Linear systems with large uncertainties, with applications to truss structures", *Reliab. Comput.* **13**:2 (2007), 149–172.

[Ngo and Tin-Loi 2007] N. S. Ngo and F. Tin-Loi, "Shakedown analysis using the p-adaptive finite element method and linear programming", *Eng. Struct.* **29**:1 (2007), 46–56.

[Nikolaidis et al. 2004] E. Nikolaidis, S. Chen, H. Cudney, R. T. Haftka, and R. Rosca, "Comparison of probability and possibility for design against catastrophic failure under uncertainty", *J. Mech. Des.* (*ASME*) **126**:3 (2004), 386–394.

[Polizzotto 1982] C. Polizzotto, "A unified treatment of shakedown theory and related bounding techniques", *Solid Mech. Arch.* **7** (1982), 19–75.

[Polizzotto et al. 1991] C. Polizzotto, G. Borino, S. Caddemi, and P. Fuschi, "Shakedown problems for material models with internal variables", *Eur. J. Mech. A Solids* **10**:6 (1991), 621–639.

[Polizzotto et al. 1993] C. Polizzotto, G. Borino, S. Caddemi, and P. Fuschi, "Theorems of restricted dynamic shakedown", *Int. J. Mech. Sci.* **35**:9 (1993), 787–801.

[Rockafellar 1970] R. T. Rockafellar, *Convex analysis*, Princeton Mathematical Series **28**, Princeton University Press, 1970.

[Schuëller and Jensen 2008] G. I. Schuëller and H. A. Jensen, "Computational methods in optimization considering uncertainties: an overview", *Comput. Methods Appl. Mech. Eng.* **198**:1 (2008), 2–13.

[Sikorski and Borkowski 1990] K. Sikorski and A. Borkowski, "Ultimate load analysis by stochastic programming", pp. 403–424 in *Mathematical programming methods in structural plasticity*, edited by D. L. Smith, CISM Courses and Lectures **299**, Springer, Wien, 1990.

[Simon and Weichert 2012] J.-W. Simon and D. Weichert, "Shakedown analysis with multidimensional loading spaces", *Comput. Mech.* **49**:4 (2012), 477–485.

[Staat and Heitzer 2003] M. Staat and M. Heitzer, "Probabilistic limit and shakedown problems", Chapter 7, pp. 217–268 in *Numerical methods for limit and shakedown analysis: deterministic and probabilistic problems*, edited by M. Staat and M. Heitzer, NIC Series **15**, John von Neumann Institute for Computing, Jülich, 2003.

[Steele 2004] J. M. Steele, *The Cauchy–Schwarz master class: an introduction to the art of mathematical inequalities*, Cambridge University Press, New York, 2004.

[Takewaki et al. 2013] I. Takewaki, K. Fujita, and S. Yoshitomi, "Uncertainties in long-period ground motion and its impact on building structural design: case study of the 2011 Tohoku (Japan) earthquake", *Eng. Struct.* **49** (2013), 119–134.

[Trần et al. 2009] T. N. Trần, R. Kraißig, and M. Staat, "Probabilistic limit and shakedown analysis of thin plates and shells", *Struct. Saf.* **31**:1 (2009), 1–18.

[Valdebenito and Schuëller 2010] M. A. Valdebenito and G. I. Schuëller, "A survey on approaches for reliability-based optimization", *Struct. Multidiscip. Optim.* **42**:5 (2010), 645–663.

[Wang et al. 1994] W. Wang, M. R. Ramirez, and R. B. Corotis, "Reliability analysis of rigid-plastic structures by the static approach", *Struct. Saf.* **15**:3 (1994), 209–235.

[Wolsey 1998] L. A. Wolsey, *Integer programming*, Wiley, New York, 1998.

[Zang et al. 2005] C. Zang, M. I. Friswell, and J. E. Mottershead, "A review of robust optimal design and its application in dynamics", *Comput. Struct.* **83**:4-5 (2005), 315–326.

YOSHIHIRO KANNO: kanno@mist.i.u-tokyo.ac.jp
Department of Mathematical Informatics, Graduate School of Information Science and Technology, University of Tokyo, Hongo 7-3-1, Bunkyo-ku, Tokyo 113-8656, Japan

JOURNAL OF MECHANICS OF MATERIALS AND STRUCTURES

Journal of Mechanics of Materials and Structures

Volume 8, No. 8-10   October-December 2013